Published OnlineFirst August 6, 2012; DOI: 10.1158/0008-5472.CAN-12-1871



# Intravesical Delivery of Small Activating RNA Formulated into Lipid Nanoparticles Inhibits Orthotopic Bladder Tumor Growth

Moo Rim Kang[1], Glen Yang[1], Robert F. Place[2], Klaus Charisse[3], Hila Epstein-Barash[3], Muthiah Manoharan[3], and Long-Cheng Li[1]

## Abstract

Practical methods for enhancing protein production *in vivo* remain a challenge. RNA activation (RNAa) is emerging as one potential solution by using double-stranded RNA (dsRNA) to increase endogenous gene expression. This approach, although related to RNA interference (RNAi), facilitates a response opposite to gene silencing. Duplex dsP21-322 and its chemically modified variants are examples of RNAa-based drugs that inhibit cancer cell growth by inducing expression of tumor suppressor $p21^{WAF1/CIP1}$ (p21). In this study, we investigate the therapeutic potential of dsP21-322 in an orthotopic model of bladder cancer by formulating a 2′-fluoro-modified derivative (dsP21-322-2′F) into lipid nanoparticles (LNP) for intravesical delivery. LNP composition is based upon clinically relevant formulations used in RNAi-based therapies consisting of PEG-stabilized unilamellar liposomes built with lipid DLin-KC2-DMA. We confirm p21 induction, cell-cycle arrest, and apoptosis *in vitro* following treatment with LNP-formulated dsP21-322-2′F (LNP-dsP21-322-2′F) or one of its nonformulated variants. Both 2′-fluoro modification and LNP formulation also improve duplex stability in urine. Intravesical delivery of LNP-dsP21-322-2′F into mouse bladder results in urothelium uptake and extends survival of mice with established orthotopic human bladder cancer. LNP-dsP21-322-2′F treatment also facilitates p21 activation *in vivo* leading to regression/disappearance of tumors in 40% of the treated mice. Our results provide preclinical proof-of-concept for a novel method to treat bladder cancer by intravesical administration of LNP-formulated RNA duplexes. *Cancer Res; 72(19); 5069–79. ©2012 AACR.*

## Introduction

Bladder cancer is the fifth most common human malignancy (1). Approximately 70% of bladder cancer incidences are diagnosed at a superficial stage in which about half will recur following transurethral resection (TUR) despite post-op therapy. Intravesical administration of chemical and/or immunologic agents (e.g., mitomycin, Bacillus Calmette-Guérin, etc.) is often used to eradicate residual tumor cells; however, such treatments can have limited efficacy and adverse side effects (2). As many as 10% to 30% of recurrent tumors will progress to a higher grade and stage inevitably forming locally invasive cancer (3, 4). Radical cystectomy remains the standard treatment of muscle-invasive bladder tumors, which often results in significant deterioration of urinary and sexual function. As such, new therapeutic options are needed for treating residual tumor after TUR, as well as advanced bladder cancer.

RNA interference (RNAi) is currently one of the leading platform technologies being developed in the clinic as an oligonucleotide-based approach to gene therapy. It is an evolutionarily conserved mechanism of gene regulation by which small double-stranded RNA (dsRNA) molecules—termed small interfering RNA (siRNA)—degrade complementary messenger RNA to silence gene expression (5). By using siRNAs as therapeutic compounds, it is possible to block the production of disease-causing proteins. However, effective uptake of siRNAs by cells requires support of a delivery vehicle to penetrate the cell membrane. Lipid-based vectors remain the preferred approach for siRNA delivery both *in vitro* and *in vivo*. Precise formulation with lipids and other molecular components (i.e., polyethylene glycol-lipid, cholesterol, etc.) allows encapsulation of siRNAs into stable liposomal nanoparticles (LNP) for improved bioavailability. Currently, ionizable lipid DLin-KC2-DMA is one of the leading materials for LNP formulation to safely deliver siRNA molecules *in vivo* (6).

Safe strategies to selectively enhance gene and/or protein production remain a challenge in gene therapy. Viral-based systems are effective at delivering exogenous constructs to facilitate gene overexpression, but have serious drawbacks (i.e.,

**Authors' Affiliations:** [1]Department of Urology and Helen Diller Comprehensive Cancer Center, University of California; [2]RNA Therapeutics Inc., San Francisco, California; and [3]Alnylam Pharmaceuticals, Inc., Cambridge, Massachusetts

**Note:** Supplementary data for this article are available at Cancer Research Online (http://cancerres.aacrjournals.org/).

M.R. Kang and G. Yang authors contributed equally to this work.

**Corresponding Author:** L-C. Li, Department of Urology and Helen Diller Comprehensive Cancer Center, University of California, San Francisco, CA. Phone: 415-476-3802; Fax: 415-514-4987; E-mail: lilc@urology.ucsf.edu

**doi:** 10.1158/0008-5472.CAN-12-1871

Published OnlineFirst August 6, 2012; DOI: 10.1158/0008-5472.CAN-12-1871



adverse effects on host genome integrity, immunologic consequences, etc.) that hinder progression in the clinic. Recently, small dsRNAs—termed small activating RNA (saRNA)—have also been shown to induce gene expression in a phenomenon referred to as RNA activation (RNAa; refs. 7, 8). Several models of RNAa have been described including transcriptional activation by targeting promoter sequences and/or overlapping noncoding regulatory transcripts using saRNA (7, 9–11). This technique offers a similar approach as RNAi, while representing a new strategy to stimulate endogenous gene expression.

The tumor suppressor protein p53 controls cell-cycle progression, senescence, and apoptosis in response to DNA damage through transactivation of numerous growth inhibitory genes (12). One such downstream target is the CDK inhibitor $p21^{WAF1/CIP1}$ (p21). By suppressing CDK activity, p21 promotes hypophosphorylation of the retinoblastoma (Rb) protein leading to cell-cycle arrest (13). In addition, p21 interacts with proliferating cell nuclear antigen (PCNA) interfering with DNA replication and cell division (14). In fact, ectopic expression of p21 has been shown to inhibit tumor growth and induce apoptosis both *in vitro* and *in vivo* (15–17). As such, p21 is a major downstream effector of p53 signaling and is itself considered a potent tumor suppressor.

Alterations to the p53 pathway represent one of the major contributors to bladder tumorigenesis (18, 19). Despite frequent disruption of the p53 protein, loss-of-function mutations leading to p21 inactivation are a rare event (20, 21). Rather, bladder cancer progression has been associated with general decreases in p21 expression (20, 21). In this regard, p21 may be an ideal target for RNAa to inhibit bladder cancer cell growth. Although the therapeutic potential of RNAa has been shown in xenograft tumors following intratumoral injection of LNP-formulated saRNA molecules (22), it has not been evaluated in a clinically relevant model of cancer using a practical route of drug administration. In the present study, we assess the antitumor activity of RNAa in an orthotopic model of bladder cancer following intravesical delivery of LNP-formulated saRNA to facilitate p21 induction. LNP composition consisted of lipid DLin-KC2-DMA and resembled RNAi-based formulations. We confirm that LNP-formulated saRNA facilitates p21 induction and possesses antiproliferative activity in bladder cancer cells. *In vivo* analyses reveal that intravesical treatment of mice with orthotopic bladder cancer extends animal survival and inhibits tumor growth. Our results provide proof-of-principle that DLin-KC2-DMA-based nanoparticles have application in delivering RNA duplexes to facilitate RNAa *in vivo*, as well as define a candidate RNAa-based drug for the treatment of localized bladder cancer by intravesical instillation.

## Materials and Methods

### Cell culture and transfection

Human bladder cancer cell line KU-7 engineered to stably express firefly luciferase and green fluorescent protein (GFP) was purchased from Caliper Life Sciences. T24-P cells are a highly tumorigenic bladder cancer subline derived from T24 cells (23) acquired from Dr. Jer-Tsong Hsieh at the University of Texas Southwestern Medical Center, Dallas, Texas. No further authentication of cell lines was done by the authors. KU-7 cells were cultured in RPMI 1640 medium supplemented with 10% fetal bovine serum (FBS) and 50 μg/mL gentamycin sulfate in a humidified atmosphere of 5% $CO_2$ at 37°C. T24-P cells were maintained in T-Medium (Invitrogen) also supplemented with 10% FBS and 50 μg/mL gentamycin sulfate. The day before transfection, cells were plated in growth medium without antibiotics at a density of ~50% to 60%. Transfection of nonformulated saRNA was carried out using Lipofectamine RNAiMAX (Invitrogen) according to manufacturer's instructions. Treatment of LNP-formulated duplexes was done by simply adding LNP solution directly to cell culture medium. The following day, transfection media was replaced with fresh media containing antibiotics. All saRNA sequences including chemical modifications are listed in Table S1.

### Lipid nanoparticle composition

Nanoparticles were prepared with the ionizable lipid 1,2-dilinoleyl-4-(2-dimethylaminoethyl)-[1,3]-dioxolane (DLin-KC2-DMA), disteroylphosphatidylcholine (DSPC), cholesterol, and 1-(monomethoxy polyethyleneglycol)-2,3-dimyristoylglycerol (PEG–DMG) using a spontaneous vesicle formation formulation procedure as previously described (24). Detailed protocol is available in Supplementary Methods.

### Urine stability assay

Solutions containing 1 μL of 20 μmol/L saRNA and 10 μL undiluted mouse or human urine were incubated at 37°C. The mixtures were flash frozen in liquid nitrogen at desired time points to halt nuclease activity until the time course was complete. Samples were subsequently mixed with loading buffer and analyzed on an agarose gel to visualize duplex levels.

### saRNA uptake analysis

T24-P cells ($1.0 \times 10^5$) were treated with LNP-formulated FITC-labeled dsP21-322-′F (dsP21-322-2′F-FITC) for 24 hours. Female C57BL/6 mice were anaesthetized with isoflurane and bladders rinsed twice with 0.2 mL PBS through a 24-guage catheter. LNP-formulated dsP21-322-2′F-FITC (1.68 mg/kg, ~33.5 μg) was administered intravesically and retained in the bladder for 2 hours by tying off the orifice of the urethra. Mice were sacrificed at 2 or 9 hours (including indwelling time) after saRNA delivery. Animals treated for 9 hours were denied water to limit excretion of formulated duplex. Whole bladders were removed, placed in cryomolds containing optimal cutting temperature compound, and frozen on dry ice. Cryostat sections were cut to 8 μm and mounted onto glass slides. Both cell and tissue slides were fixed in 10% neutral buffered formalin and washed with PBS containing sucrose. The fixed sections were counterstained with 4′,6-diamidino-2-phenylindole (DAPI) using VECTASHIELD Mounting Medium (Vector Laboratories) and saRNA uptake was visualized using fluorescence microscopy.

### Orthotopic model of bladder cancer and intravesical treatment

The animal study was carried out according to a protocol approved by the Institutional Animal Care and Use Committee. The orthotopic murine model of bladder cancer was a

Published OnlineFirst August 6, 2012; DOI: 10.1158/0008-5472.CAN-12-1871



modification of a previously described technique (25, 26). In brief, female nude (nu/nu) mice at 8 to 10 weeks of age (Simonsen Laboratory) were anaesthetized with isoflurane. Chemical lesions to the bladder urothelium were carried out by injecting 10 μL of 0.5 M silver nitrate into the bladder of each animal through a 24-gauge catheter. Bladders were washed with PBS and subsequently instilled with KU-7 cells ($2.0 \times 10^6$) suspended in 50 μL PBS via catheter. At this point, animals were dosed with ketamine (100 mg/kg) and xylazine (10 mg/kg) by intraperitoneal injection. Cells were retained in the bladder for 2 hours by tying off the orifice of the urethra. One day following tumor cell implantation, *in vivo* bioluminescence imaging (BLI) of KU-7 cells was evaluated on a IVIS Spectrum Imaging System (Caliper Life Sciences) following intraperitoneal administration of 150 mg/kg D-luciferin (Gold Biotechnology). Bioluminescence signal (BLS) was acquired and analyzed using Living Image software version 4.10 (Xenogen). Regions of interest (ROI) were defined manually to encompass the bladder and quantify signal intensity. Tumor-bearing mice were randomly divided into 3 treatment groups (PBS, LNP-dsCon-2′F, and LNP-dsP21-322-2′F) each containing 9 to 10 animals. Mice received 3 mg/kg of LNP-formulated duplex in a volume of 50 μL by intravesical administration into the bladder via catheter. Each treatment was retained in the bladder for 2 hours by tying off the orifice of the urethra while the animal was anaesthetized. PBS treatments were done at volumes equivalent to LNP-dsP21-322-2′F doses. Animals were treated 14 total times every 3 days beginning at day 4 postimplantation. BLS and body weight were monitored weekly. A death was recorded if animals met AVMA guidelines for euthanasia as a result of tumor burden including body condition score (BCS) $\leq 2$ and $\geq 20\%$ weight loss. The study was terminated 8 weeks following tumor installation. Any surviving mice were euthanized and all major organs including bladders were inspected for cancer. Bladder tumor tissue was divided in half and placed in either RIPA buffer containing protease inhibitors or 10% neutral buffered formalin for immunoblot analysis or immunohistochemistry (IHC), respectively.

### Statistical analyses

The differences in continuous variables between treatments were assessed by Student *t* test (for 2 treatments) or ANOVA (for 3 or more treatments). Log rank tests determined statistical significance of Kaplan–Meier survival curves. Significance was defined as $P < 0.05$. Additional experimental procedures are described in Supplementary Methods.

## Results

### dsP21-322 induces p21 expression in human bladder cancer cells

By screening several duplexes targeting the p21 promoter, dsP21-322 has been identified as a lead saRNA molecule with antitumor activity in prostate cancer (22). Earlier *in vitro* studies have showed that dsP21-322 also possesses growth inhibitory function in T24 and J82 bladder cancer cell lines (27). To further evaluate dsP21-322 activity in bladder cancer, we transfected KU-7 and T24-P cells with dsP21-322 for 72 hours. Analysis of mRNA expression revealed that dsP21-322 profoundly induced p21 levels compared with mock and nonspecific control (dsCon) treatments (Fig. 1A). Induction of p21 was further confirmed by immunoblot analysis. As shown in Fig. 1B, elevated levels of p21 protein correlate to the increase in p21 mRNA expression. Morphologically, dsP21-322 treatment caused cells to appear less dense and acquire larger, more flattened shapes; phenotypes indicative of impeded cell growth (Fig. S1). These results imply dsP21-322 retains RNAa activity and growth inhibitory function in KU-7 and T24-P cells.

### Activity of LNP-formulated dsP21-322-2′F and its nonformulated variants

Chemical modification (e.g., 2′-fluoro) is often required to improve the medicinal properties of duplex RNAs for *in vivo* application (28). We previously defined a chemically modified variant of dsP21-322 (dsP21-322-2′F) with improved nuclease resistance in serum and reduced immunostimulatory activity by introducing 2′-fluoro modifications to all pyrimidine nucleotides in its antisense strand (22). To further improve its *in vivo* applicability, we formulated dsP21-322-2′F into lipid nanoparticles (LNP-dsP21-322-2′F) composed of ionizable lipid DLin-KC2-DMA creating PEG-stabilized unilamellar liposomal vesicles. Nonspecific lipid-based nanoparticles (LNP-dsCon-2′F) were also formulated as a control. Comparative analysis of *in vitro* potency between nonformulated dsP21-322 and dsP21-322-2′F in KU-7 cells revealed similar $EC_{50}$ (half maximal effective concentration) values of 1.42 and 1.70 nmol/L at 72 hours, respectively (Fig. 1C). In addition, dsP21-322-2′F retained strong RNAa activity as compared with dsP21-322. As shown in Fig. 1C, dsP21-322-2′F consistently increased p21 levels by ~9-fold at maximal activity, whereas dsP21-322 increased p21 levels by ~5-fold. Dose-response experiments with LNP-dsP21-322-2′F indicated an $EC_{50}$ of 0.24 μg/mL with maximal activity reaching ~10-fold increases in p21 levels (Fig. 1C). Immunoblot analyses also revealed dose-dependent induction of p21 protein by dsP21-322, dsP21-322-2′F, and LNP-dsP21-322-2′F (Fig. 1D). We conducted dose–response experiments evaluating cell viability by MTS assay and calculated $IC_{50}$ (half maximal inhibitory concentration) values to measure the antiproliferative potency of LNP-dsP21-322-2′F and its nonformulated variants. Nonformulated dsP21-322 and dsP21-322-2′F had similar $IC_{50}$ values of 0.72 and 0.74 nmol/L, respectively; whereas LNP-dsP21-322-2′F had an $IC_{50}$ of 0.19 μg/mL at 72 hours (Fig. S2A). Phenotypically, dsP21-322-2′F and LNP-dsP21-322-2′F treatments caused dose-dependent changes in cell morphology and density similar to dsP21-322 (Fig S2B). Taken together, these results indicate that neither chemical modification nor LNP formulation negatively impacted RNAa activity or the growth inhibitory function of dsP21-322.

### LNP-formulated dsP21-322-2′F and its nonormulated variants cause cell-cycle arrest and apoptosis in bladder cancer cells

To investigate cell-cycle distribution, DNA content was analyzed by flow cytometry in cells stained with propidium iodide (PI) following treatment with LNP-dsP21-322-2′F or one

Published OnlineFirst August 6, 2012; DOI: 10.1158/0008-5472.CAN-12-1871



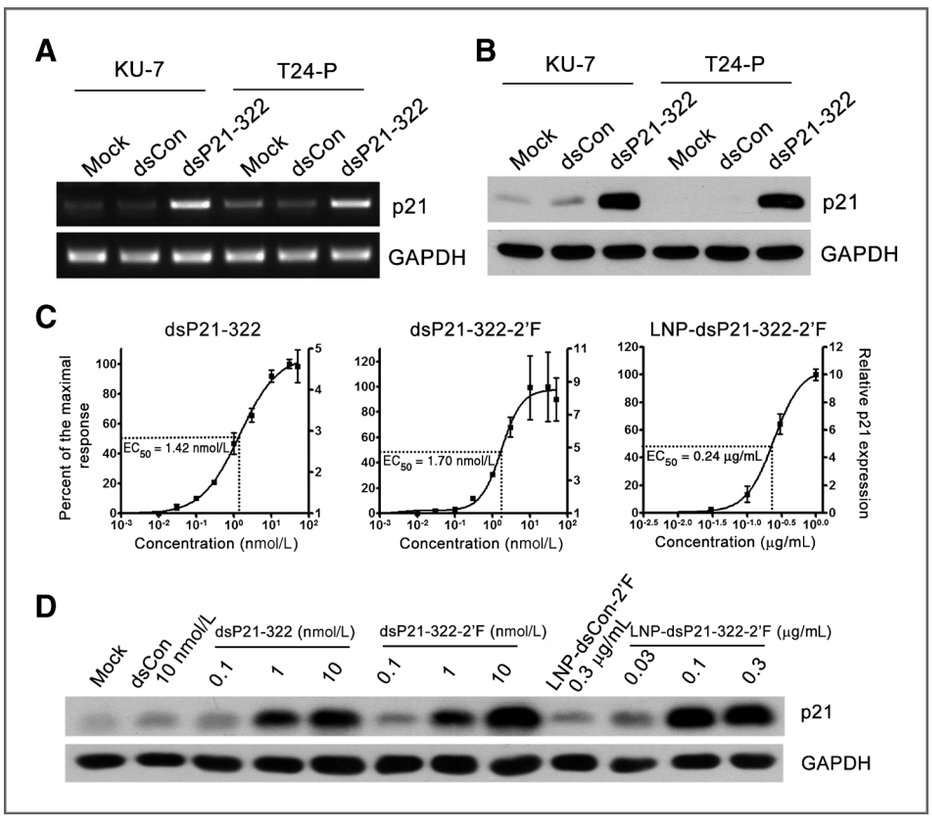


**Figure 1.** Activity of LNP-dsP21-322-2′F and its nonformulated derivatives in bladder cancer cells. A, human KU-7 and T24-P cells were transfected with 50 nmol/L of the indicated duplexes for 72 hours. Mock samples were transfected in the absence of dsRNA. Semiquantitative RT-PCR was used to assess p21 and GAPDH mRNA levels. Amplification of GAPDH served as a loading control. B, protein levels of p21 and GAPDH were evaluated by immunoblot analysis using protein-specific antibodies. C, KU-7 cells were treated with accumulating concentrations of dsP21-322, dsP21-322-2′F, and LNP-dsP21-322-2′F for 72 hours. Expression of p21 was quantified by real-time PCR (mean ± SD from 2 independent experiments). Maximum and minimum levels of induction correlate to 100% and 0% response, respectively. Duplex (nmol/L) and nanoparticle (μg/mL) concentration are shown in log scale. Dotted lines illustrate approximate $EC_{50}$ values. D, KU-7 cells were transfected at the indicated concentrations of formulated (LNP-dsCon-2′F and LNP-dsP21-322-2′F) or nonformulated (dsCon, dsP21-322, and dsP21-322-2′F) duplex for 72 hours. Protein levels of p21 and GAPDH were evaluated by immunoblot analysis using protein-specific antibodies. Concentrations of LNP-dsP21-322-2′F (μg/mL) correspond to total nanoparticle, whereas dsP21-322 and dsP21-322-2′F treatments represent concentrations (nmol/L) of only the individual duplexes. Data are representative of $n = 3$.

of its variants. As shown in Fig. 2A and B, transfection of dsP21-322 or dsP21-322-2′F caused $G_0$–$G_1$ arrest in KU-7 cells as indicated by the increase in $G_0$–$G_1$ cell number and concurrent declines in S and $G_2$–M populations. LNP-dsP21-322-2′F treatment also caused changes in cell-cycle distribution similar to dsP21-322 and dsP21-322-2′F corroborating that LNP formulation did not interfere with the growth inhibitory function of dsP21-322-2′F (Fig. 2A and B).

Cell-cycle arrest by p21 is primarily mediated although inhibition of CDK activity leading to Rb hypophosphorylation (22, 29). As such, we evaluated phosphorylated Rb (p-Rb) levels in KU-7 cells following treatment with dsP21-322, dsP21-322-2′F or LNP-dsP21-322-2′F. As shown in Fig. 2C, transfection with nonformulated dsP21-322 and dsP21-322-2′F reduced p-Rb levels in a dose-dependent manner, whereas total Rb protein remained generally unchanged. Similarly, LNP-dsP21-322-2′F treatment also reduced p-Rb levels at elevated doses (Fig. 2C). These data suggest that p21 induction resulted in a functional protein capable of manipulating Rb phosphorylation.

Overexpression of p21 has been reported to have proapoptotic function in several cancer cell types contributing to its tumor suppressor activity (12, 27, 30). To quantify the apoptotic cell fraction following duplex treatments, KU-7 cells were analyzed by flow cytometry following staining with 7-AAD and Annexin V-PE. As shown in Fig. 3A and B, mock and dsCon treatments defined baseline apoptosis in KU-7 cells, whereas transfection with dsP21-322 or dsP21-322-2′F caused similar dose-dependent increases in early and late stage apoptosis. LNP-dsCon-2′F mirrored nonformulated control treatments; however, LNP-dsP21-322-2′F caused robust detection of early and late stage apoptotic cells in a dose-dependent manner similar to dsP21-322 and dsP21-322-2′F transfections (Fig. 3A and B). We also measured caspase-3/7 activity (2 key enzymes of the apoptotic signaling cascade) in culture media following duplex treatments. Transfection of dsP21-322 or dsP21-322-2′F possessed significantly higher caspase-3/7 activity than control treatments (Fig. 3C). Likewise, LNP-dsP21-322-2′F caused similar increases in caspase 3/7 signaling, whereas LNP-dsCon-2′F treatment had nominal effects on caspase-3/7 activity (Fig. 3C).

Published OnlineFirst August 6, 2012; DOI: 10.1158/0008-5472.CAN-12-1871



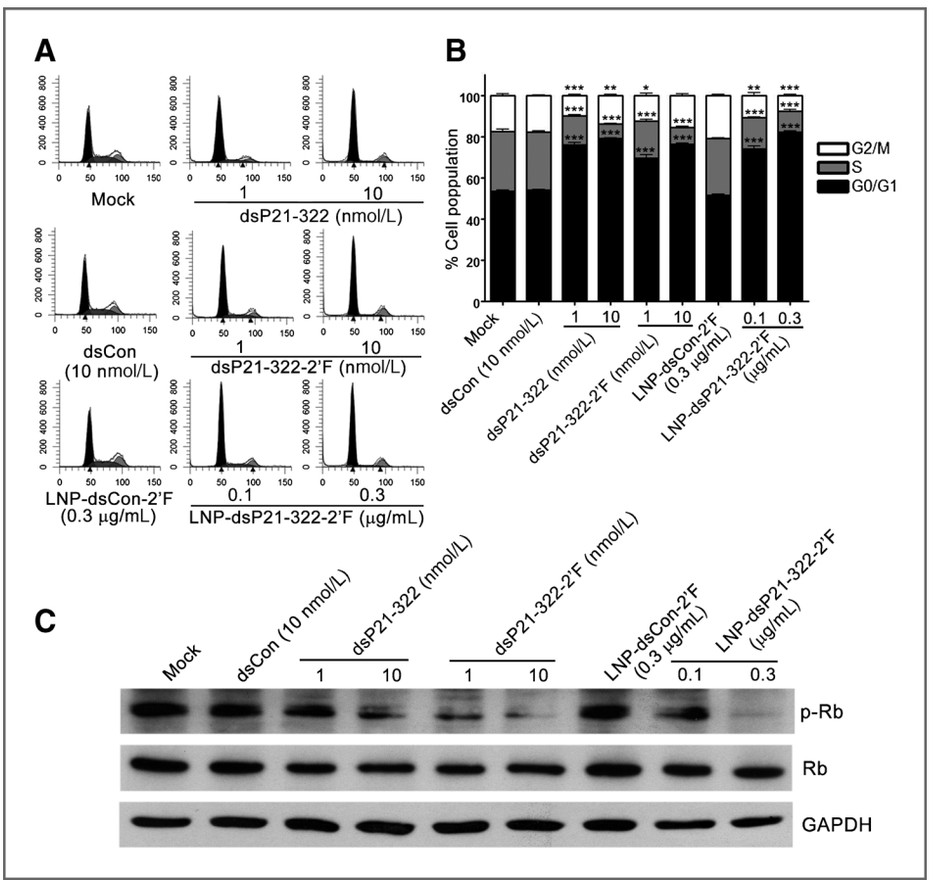


**Figure 2.** LNP-dsP21-322-2′F and its nonformulated derivatives promote cell cycle arrest and Rb hypophosphorylation. A, KU-7 cells were treated at the indicated concentrations of formulated (LNP-dsCon-2′F and LNP-dsP21-322-2′F) or nonformulated (dsCon, dsP21-322, and dsP21-322-2′F) duplex for 72 hours and analyzed by flow cytometry after PI staining. Shown are examples of resulting FL2A histograms. B, flow cytometry data were analyzed to determine cell cycle distribution (mean ± SD from 2 independent experiments). Percentages correspond to the amount of cells present in the treatment populations at the indicated phases of cell cycle ($G_0$–$G_1$, S, or $G_2$–M). *, $P < 0.05$; **, $P < 0.01$; ***, $P < 0.001$. C, protein levels of phosphorylated Rb (p-Rb), total Rb (Rb), and GAPDH were determined by immunoblot analysis. GAPDH served as a loading control.

Immunoblot analysis was also carried out to monitor reductions in procaspase-3 levels (a marker for caspase-3 activation) and cleavage of PARP (a downstream substrate of caspase signaling). Transfection with dsP21-322 or dsP21-322-2′F led to reductions in procaspase-3 (caspase-3) with concurrent detection of PARP cleavage (Fig. 3D). Similarly, LNP-dsP21-322-2′F mirrored nonformulated transfection results (Fig. 3D). Taken together, these results indicate that treatment with LNP-dsP21-322-2′F or its nonformulated variants also promote apoptosis contributing to the antitumor activity in bladder cancer cells.

### Pharmacokinetic properties of LNP-formulated dsP21-322-2′F

Urine is a liquid waste product excreted by the kidney and stored in the bladder that is rich in nucleases including ribonucleases (31). To test the stability of LNP-dsP21-322-2′F and its nonformulated derivatives in urine, we incubated equal quantities of duplex with fresh human or mouse urine for up to 6 days. Unmodified dsP21-322 was generally unstable in human urine having completed degraded within 3 hours; however, 2′-fluoro modification of dsP21-322 (dsP21-322-2′F) significantly increased duplex stability extending its life to ∼24 hours (Fig. 4A). Packaging RNA into nanoparticles has also been shown to protect encapsulated cargo from degradation by nucleases (32). As such, LNP formulation further improved its nuclease resistance increasing its stability to ∼6 days in human urine. Surprisingly, duplex stability behaved very different in mouse urine. Almost no apparent degradation of unmodified, modified, or LNP-formulated saRNA was observed (Fig. 4A). Stability studies in sterile water resembled the time course in mouse urine suggesting nominal ribonuclease activity and/or inherent duplex stability in mouse urine (Fig. S3A). In support, analysis of untreated mouse urine yielded stable background detection of low molecular weight nucleic acids, whereas human urine was devoid of any inherent nucleic acid signal (Fig. S3B). These data indicate that both 2′fluoro modification and LNP formulation improve duplex stability in human urine; however, inherent differences in nuclease activity/composition between human and mouse urine may influence *in vivo* properties in either species.

To assess *in vitro* and *in vivo* uptake of LNP-formulated saRNA, FITC was conjugated to the 3′ terminus of dsP21-322-2′F (dsP21-322-2′F-FITC) and formulated into unilamellar LNP vesicles with DLin-KC2-DMA. When LNP-formulated dsP21-322-2′F-FITC was directly added to cultured cells, uptake was evident in nearly all cells with fluorescence mainly localized to the cytoplasm and a few punctate nuclear loci at 24 hours (Fig. 4B). *In vivo* uptake was evaluated by directly treating the bladders of normal mice with LNP-formulated dsP21-322-2′F-FITC via intravesical administration. After 2 hours of treatment, dsP21-322-2′F-FITC uptake was observed in cells

Published OnlineFirst August 6, 2012; DOI: 10.1158/0008-5472.CAN-12-1871



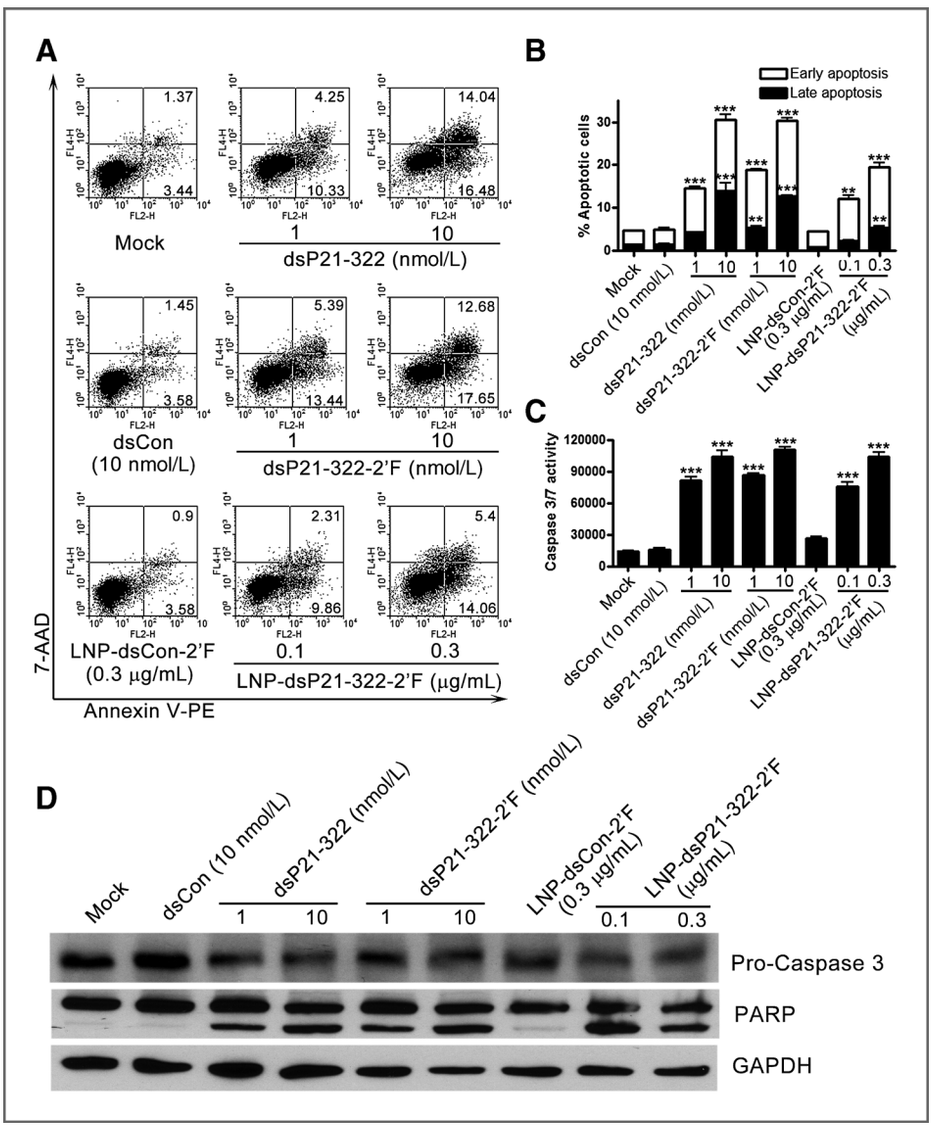


**Figure 3.** LNP-dsP21-322-2′F and its nonformulated derivatives promote apoptosis. A, KU-7 cells were treated at the indicated concentrations of formulated (LNP-dsCon-2′F and LNP-dsP21-322-2′F) or nonformulated (dsCon, dsP21-322, and dsP21-322-2′F) duplex for 72 hours and analyzed by flow cytometry after staining with 7-AAD and Annexin V-PE. Shown are examples of resulting scatters plots with indicated quadrant percentages corresponding to early and late stage apoptosis. B, flow cytometry data were plotted to compare apoptotic cell populations in each treatment (mean ± SD from 3 independent experiments). Percentages correspond to the amount of cells in early or late stage apoptosis. C, caspase-3/7 activity was determined by measuring luminescence of a cleavable reporter substrate. Data are plotted as the mean ± SD from 3 independent experiments. *, $P < 0.05$; **, $P < 0.01$; ***, $P < 0.001$. D, levels of procaspase-3 (caspase-3), PARP, and GAPDH were evaluated by immunoblot analysis. Detection of a lower molecular product signifies PARP cleavage.

lining the inner bladder wall, as well as the interstitial spaces of the urothelium (Fig. 4C). Fluorescence remained readily detectable in bladder cells by 9 hours (Fig. 4D). Images taken at higher magnification clearly show intracellular distribution of dsP21-322-2′F-FITC at 2 and 9 hours (Fig. S4). These data indicate that LNP formulation effectively delivers saRNA duplex into the bladder epithelium.

### Intravesical treatment of LNP-dsP21-322-2′F inhibits growth of orthotopic bladder tumors

To test the antitumor activity of LNP-dsP21-322-2′F *in vivo*, we established orthotopic bladder cancer in 40 immunocompromised (nu/nu) mice by intravesical instillation of KU-7 cells. BLS from KU-7 cells was detected by measuring photons/second following intraperitoneal administration of luciferase substrate (D-luciferin). The day following tumor cell instillation, 29 mice (72.5%) produced BLS and were randomly divided into 3 treatment groups including PBS ($n = 9$), LNP-dsCon-2′F ($n = 10$), and LNP-dsP21-322-2′F ($n = 10$). No statistical difference in BLS intensity or body weight was detected between groups at time of randomization. Intravesical treatment was initiated on day 4 postimplantation and repeated every 3 days for 14 total doses (Fig. 5A). BLI was done weekly to monitor tumor burden. Animal survival was the primary endpoint.

At the end of the 8 week study, the median survival time for PBS, LNP-dsCon-2′F, and LNP-dsP21-322-2′F treatment groups was 9, 13, and 45 days, respectively. Five mice (50%) remained alive in the LNP-dsP21-322-2′F population, whereas 1 mouse (11%) survived in the PBS group and none (0%) represented LNP-dsCon-2′F-treated animals. Kaplan–Meier cumulative survival analysis revealed LNP-dsP21-322-2′F treatment significantly extended animal survival compared with PBS and LNP-dsCon-2′F, whereas no significant difference was detected between the 2 control groups (Fig. 5B). Four of the surviving mice in the LNP-dsP21-322-2′F treatment population

Published OnlineFirst August 6, 2012; DOI: 10.1158/0008-5472.CAN-12-1871



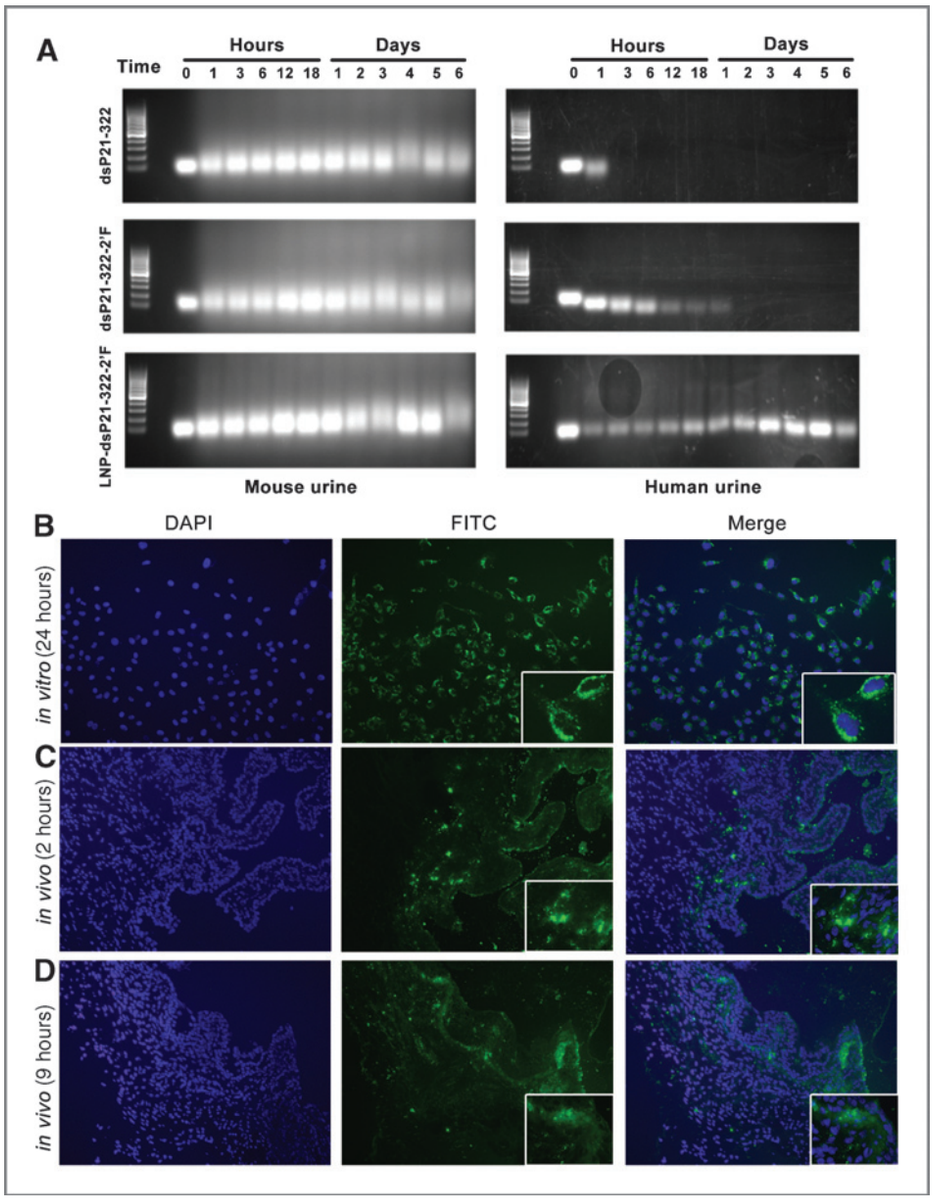


**Figure 4.** Urine stability and intracellular uptake of LNP-dsP21-322-2′F. A, equal quantities of dsP21-322, dsP21-322-2′F, and LNP-dsP21-322-2′F were incubated in mouse or human urine for the indicated lengths of time. Duplex stability was visualized on an agarose gel. B, T24-P cells were treated with LNP-formulated dsP21-322-2′F-FITC (0.3 μg/mL) for 24 hours. Cells were subsequently fixed, counterstained with DAPI (blue), and analyzed by fluorescent microscopy to visualize intracellular uptake of dsP21-322-2′F-FITC *in vitro* (green). C and D, one dose (~33.5 μg) of LNP-formulated dsP21-322-2′F-FITC was instilled by intravesical administration into the bladder of normal mice and kept indwelling for 2 hours. Bladders were surgically removed at 2 hours (C) or 9 hours (D) following instillation for cryosectioning. Tissue sections were counterstained with DAPI and visualized by fluorescent microscopy. All images were taken at equal exposure times. Representative images of *in vivo* dsP21-322-2′F-FITC uptake (green) and nuclear staining (DAPI, blue) in bladder tissue are shown at 2 hours (C) and 9 hours (D). Insets contain enlarged images of fluorescent staining.

showed gradual reductions in tumor burden in which 3 eventually became tumor-free as evidenced by the disappearance in BLS (Fig. 6A and B). Removal and dissection of tumor-free bladders were devoid of GFP signal upon inspection by fluorescence microscopy to further suggest tumor disappearance (Fig. S5). In one of the tumor-free animals, a white area of scarred tissue with negative GFP signal was found in the bladder wall suggesting regression of an established tumor (Fig. S5). Similar observations have been noted following regression of prostate xenograft tumors treated with dsP21-322-2′F formulated into lipidoid-based nanoparticles (22). Histologic evaluation revealed in some instances that orthotopic tumor from control groups invaded into the bladder detrosal muscle layer (Fig. S6A). In addition, kidney metastases were found in 2 of 9, 1 of 10, and 3 of 10 mice within the PBS, LNP-dsCon-2′F and LNP-dsP21-322-2′F treatment groups, respectively (Fig. S6B). No metastases in other organs were noted.

IHC analysis of harvested mouse bladders revealed strong nuclear staining for p21 in LNP-dsP21-322-2′F-treated tumors as compared with PBS and LNP-dsCon-2′F control tissue (Fig. 7A). Detection of cleaved caspase 3 also revealed increased activation in LNP-dsP21-322-2′F-treated tumors indicative of apoptosis (Fig. 7A). Hematoxylin and eosin (H&E) staining and Ki67 detection were used to identify orthotopic tumor in the tissue slides (Fig. 7A). Increased levels of p21 protein were also evaluated by immunoblot analysis in protein extracts prepared from total homogenized tissue (Fig. 7B). Densitometry analysis measured ~3.3- to 5.2-fold increase in p21 levels within LNP-dsP21-322-2′F-treated tissue (Fig. 7C). These results confirm *in*

Published OnlineFirst August 6, 2012; DOI: 10.1158/0008-5472.CAN-12-1871



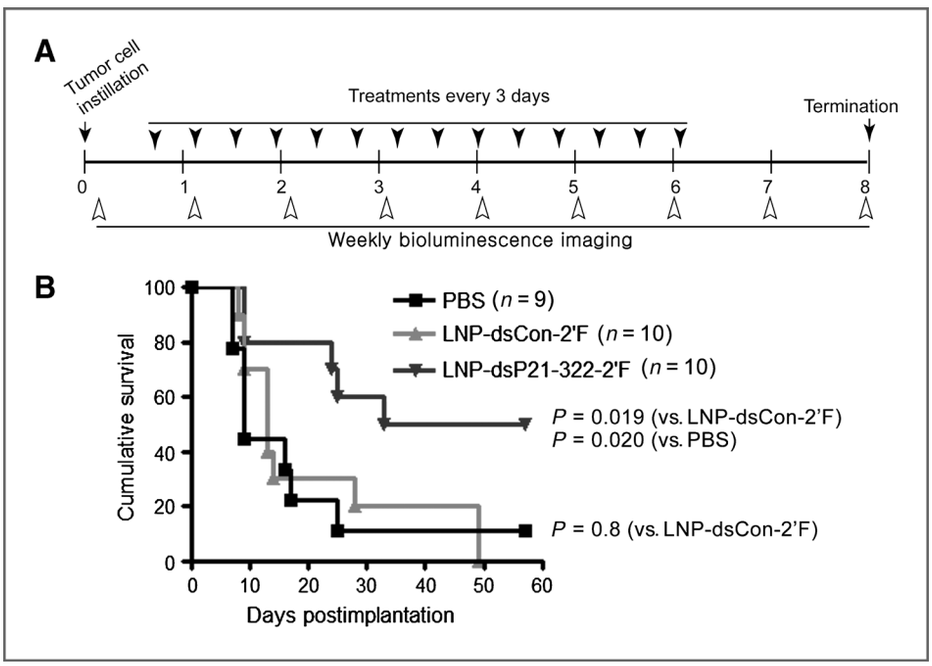


**Figure 5.** Intravesical delivery of LNP-dsP21-322-2′F extends survival of mice with orthotopic human bladder cancer. A, schematic diagram of study design and dosing schedule. Treatments began 4 days postimplantation for 14 total doses every 3 days (solid arrowheads). BLI of mouse bladders was done weekly (open arrowheads). B, mouse survival in the days following tumor implantation was monitored in PBS, LNP-dsCon-2′F, and LNP-dsP21-322-2′F treatment groups. Data are plotted as Kaplan–Meier cumulative survival curves.

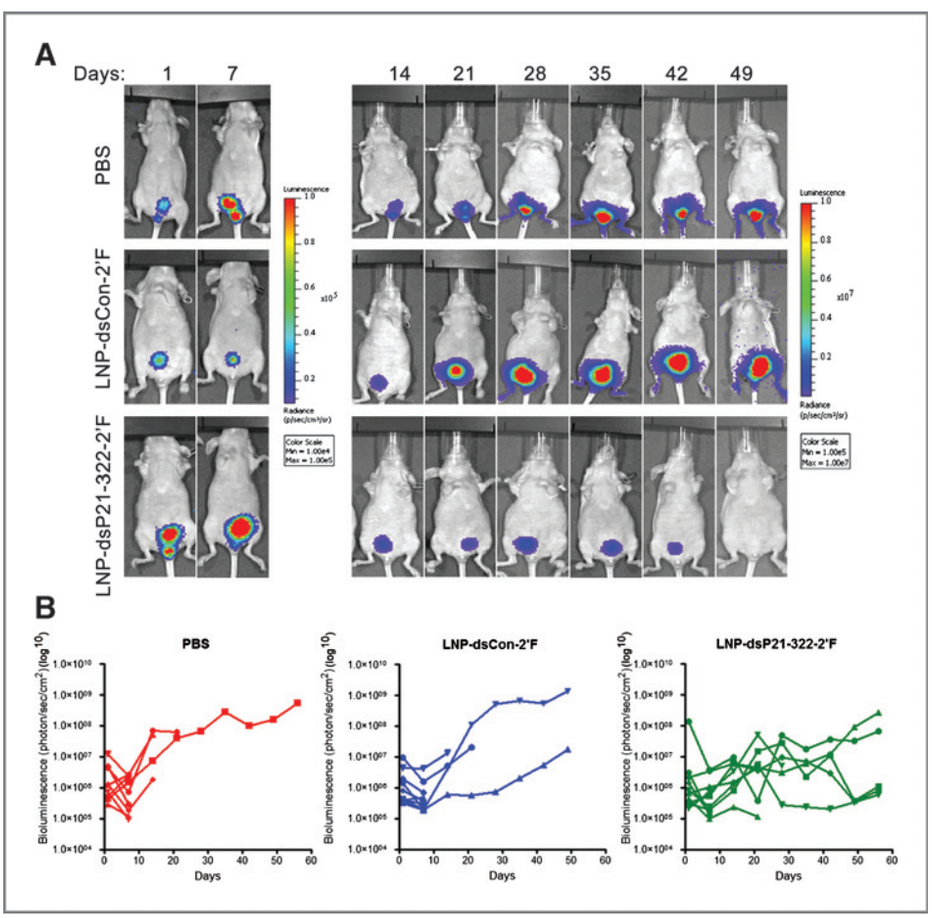


**Figure 6.** Intravesical delivery of LNP-dsP21-322-2′F inhibits orthotopic bladder tumor growth. A, cancer growth was monitored by evaluating bladder tumor bioluminescence over the lifespan of each animal. Shown are BLI images of a representative mouse from each treatment group (PBS, LNP-dsCon2′F, or LNP-dsP21-322-2′F) at the indicated time points (days). Note normalization of BLS intensities at days 1 and 7 differed from days 14 to 49 in order for tumor signals to fall within the limits of scale. B, tumor bioluminescence within each mouse bladder is plotted over animal lifespan for all treatment groups. Note the general trend of tumor bioluminescence in PBS and LNP-dsCon-2′F treatment groups increases with time, whereas bioluminescence in animals treated with LNP-dsP21-322-2′F collectively remains flat. Background signal generated by ROIs in tumor-free animals of the LNP-dsP21-322-2′F group were still plotted on the *Y*-axis (Bioluminescence) to prevent line termination and improper interpretation as animal death.

Published OnlineFirst August 6, 2012; DOI: 10.1158/0008-5472.CAN-12-1871



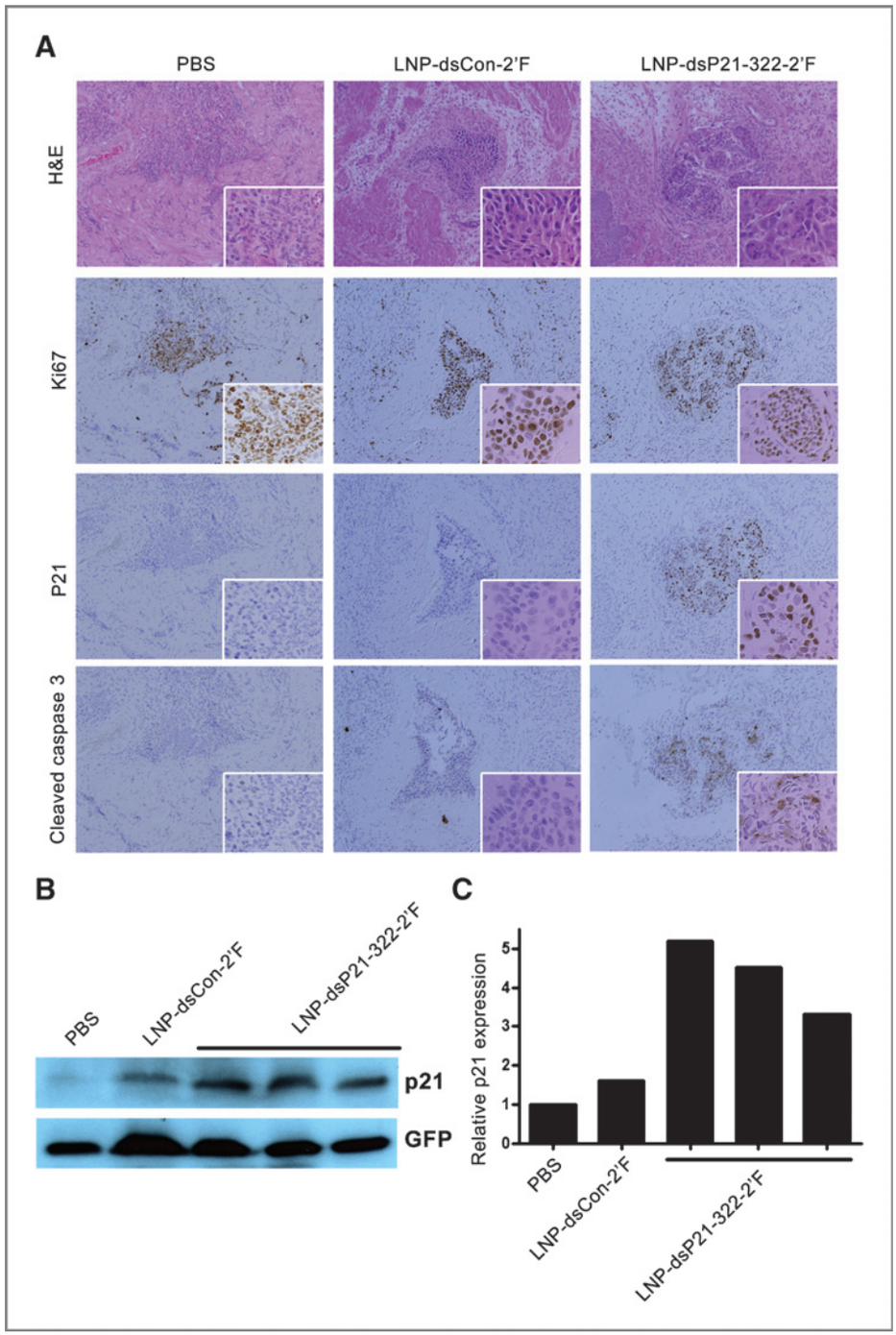


**Figure 7.** LNP-dsP21-322-2′F induces p21 in orthotopic bladder tumors. A, representative H&E immunohistochemical staining of Ki67, p21, and cleaved caspase-3 in tissue slides prepared from PBS, LNP-dsCon-2′F, and LNP-dsP21-322-2′F-treated murine bladders. H&E staining and Ki67 detection were carried out to identify orthotopic tumors. Insets are enlarged images of tumor cells. Note nuclear staining for p21 and Ki67. B, whole bladder tissue was homogenized and p21 induction was confirmed by immunoblot analysis. Detection of GFP served as a loading control. Samples of LNP-dsP21-322-2′F treatments are from 3 separate bladders.C, relative expression of p21 was quantified by densitometry analysis of the immunoblot in B. The amounts of p21 protein were normalized to GFP levels.

*vivo* activation of p21 expression in orthotopic tumors by intravesical administration of LNP-dsP21-322-2′F.

## Discussion

We previously showed that dsP21-322 possesses *in vitro* antigrowth activity in T24 and J82 bladder cancer cell lines (27). In the present study, we implement a chemically-modified variant of dsP21-322 (dsP21-322-2′F) with improved nuclease resistance and reduced immunostimulatory activity to improve its pharmaceutical properties for *in vivo* application (22). In addition, we use a clinically relevant LNP delivery system currently being implemented for RNAi-based therapies to achieve intracellular uptake of dsP21-322-2′F in target tissue. Intravesical administration of LNP-formulated dsP21-322-2′F (LNP-dsP21-322-2′F) into murine bladders with

Published OnlineFirst August 6, 2012; DOI: 10.1158/0008-5472.CAN-12-1871



orthotopic cancer inhibited tumor growth and extended animal survival. Our results provide proof-of-principle that targeted gene induction via RNAa in conjunction with current delivery platforms may represent a novel approach to treat bladder cancer.

Two previous studies in mice have reported the antitumor effects of siRNA delivered intravesically by targeting PLK1 and survivin (33, 34). Because these studies used only a limited number of animals, tumor burden served as the primary end point. To assess treatment efficacy, we opted to use animal survival as the primary end point, whereas monitoring tumor response by BLS throughout the study. To achieve sufficient statistical power, we used a large population containing 29 animals with established orthotopic bladder tumors (9 to 10 mice/group). In fact, this study currently represents the largest cohort of animals ever used to evaluate small RNA-based therapeutics in an orthotopic bladder cancer model. We observed that intravesical delivery of LNP-dsP21-322-2′F caused regression/disappearance of tumors in 40% of the treated mice and significantly prolonged animal survival compared with control groups. As such, LNP-dsP21-322-2′F may represent a putative intravesical drug for treating bladder cancer and controlling recurrence.

KU-7 cells have been used to establish orthotopic bladder tumors in immunocompromised mice (26, 35). A previous study indicated that KU-7 tumors are confined to the lamina propria within 4 weeks (35); however, we observed muscle invasion at longer periods of observation ($\geq$4 weeks). In some instances, metastases were found in the kidney, which most likely resulted from retrograde migration of the instilled tumor cells. Such metastases also seemed to evade treatment delivered locally to the bladder. In our hands, KU-7 cells not only modeled superficial bladder cancer, but also recapitulated muscle-invasive and metastatic disease.

The target site of dsP21-322 is not shared between mouse and human due to poor conservation of p21 promoter sequence (36). As such, it is currently unknown whether p21 induction by dsP21-322-2′F poses adverse effects to the normal bladder epithelium in humans. RNAa is a bias mechanism of gene overexpression in which some cell lines/types can be resistant to saRNA treatment. In some cases, highly downregulated genes are more sensitive to gene activation. Because p21 is associated with reduced expression in bladder cancer (20, 21), it may possess an innate susceptibility to RNAa; whereas normal bladder cells may be more resilient to p21 induction by dsP21-322-2′F. In this regard, LNP-dsP21-322-2′F may possess an inherent bias toward disease tissue. Nonetheless, further evaluation of dsP21-322-2′F needs to be done to identify its effects on normal tissue health.

Intravesical administration of small RNA drugs has the advantage of bringing high concentrations of drug into direct contact with diseased tissue without the side effects associated with systemic drug administration. The dosing schedule used in our study mirrors current treatment regimens for intravesical immunotherapy Bacillus Calmette-Guerin (BCG), which is used to treat superficial and recurrent bladder cancer in humans. Furthermore, we used a clinically relevant unilamellar LNP to improve the bioavailability of dsP21-322-2′F. LNP-formulation drastically enhanced dsP21-322-2′F stability in urine and capacity to penetrate the protective glycosaminoglycan (GAG) layer of the bladder delivering duplex to the underlying urothelial cells. In summary, we show that LNP-dsP21-322-2′F has antitumor activity in an orthotopic model of bladder cancer by elevating p21 levels *in vivo*. Our results provide preclinical proof-of-concept that DLin-KC2-DMA-based nanoparticles have application in delivering RNA duplexes to facilitate RNAa *in vivo*, as well as define a candidate RNAa-based drug for the treatment of regional bladder cancer that may have clinical relevance as an adjuvant therapy after TUR.

## Disclosure of Potential Conflicts of Interest

R.F. Place is employed at RNA Therapeutics. K. Charisse, H. Epstein-Barash, M. Manoharan are employees at Alnylam Pharmaceuticals. L-C. Li and R.F. Place are named inventors on pending patent applications related to RNAa, which have been filed by the University of California San Francisco and licensed to Alnylam Pharmaceuticals. No potential conflicts of interest were disclosed by the other authors.

## Authors' Contributions

**Conception and design:** M.R. Kang, M. Manoharan, L-C. Li
**Development of methodology:** M.R. Kang, R.F. Place, H. Epstein-Barash, M. Manoharan, L-C. Li
**Acquisition of data (provided animals, acquired and managed patients, provided facilities, etc.):** M.R. Kang, K. Charisse
**Analysis and interpretation of data (e.g., statistical analysis, biostatistics, computational analysis):** M.R. Kang, R.F. Place, L-C. Li
**Writing, review, and/or revision of the manuscript:** M.R. Kang, R.F. Place, K. Charisse, M. Manoharan, L-C. Li
**Administrative, technical, or material support (i.e., reporting or organizing data, constructing databases):** R.F. Place, L-C. Li
**Study supervision:** R.F. Place, M. Manoharan, L-C. Li
**Developed the formulation used for the study:** H. Epstein-Barash

## Acknowledgments

We would like to thank Dr. Jer-Tsong Hsieh at the Department of Urology, University of Texas Southwestern Medical Center for his generous support with the bladder cancer model. This work is supported by the AACR Henry Shepard Bladder Cancer Research Grants (09-60-30-LI).

The costs of publication of this article were defrayed in part by the payment of page charges. This article must therefore be hereby marked *advertisement* in accordance with 18 U.S.C. Section 1734 solely to indicate this fact.

Received May 21, 2012; revised July 26, 2012; accepted July 28, 2012; published OnlineFirst August 6, 2012.

## References

1. American Cancer Society. Cancer Facts & Figures 2012. Atlanta: American Cancer Society; 2012.
2. Shen Z, Shen T, Wientjes MG, O'Donnell MA, Au JL. Intravesical treatments of bladder cancer: review. Pharm Res 2008;25:1500–10.
3. Gee J, Sabichi AL, Grossman HB. Chemoprevention of superficial bladder cancer. Crit Rev Oncol Hematol 2002;43:277–86.
4. Cookson MS, Herr HW, Zhang ZF, Soloway S, Sogani PC, Fair WR. The treated natural history of high risk superficial bladder cancer: 15-year outcome. J Urol 1997;158:62–7.
5. Fire A, Xu S, Montgomery MK, Kostas SA, Driver SE, Mello CC. Potent and specific genetic interference by double-stranded RNA in Caenorhabditis elegans. Nature 1998;391:806–11.

Published OnlineFirst August 6, 2012; DOI: 10.1158/0008-5472.CAN-12-1871




6. Huang L, Liu Y. In vivo delivery of RNAi with lipid-based nanoparticles. Annu Rev Biomed Eng 2011;13:507–30.
7. Li LC, Okino ST, Zhao H, Pookot D, Place RF, Urakami S, et al. Small dsRNAs induce transcriptional activation in human cells. Proc Natl Acad Sci U S A 2006;103:17337–42.
8. Janowski BA, Younger ST, Hardy DB, Ram R, Huffman KE, Corey DR. Activating gene expression in mammalian cells with promoter-targeted duplex RNAs. Nat Chem Biol 2007;3:166–73.
9. Place RF, Noonan EJ, Foldes-Papp Z, Li LC. Defining features and exploring chemical modifications to manipulate RNAa activity. Curr Pharm Biotechnol 2010;11:518–26.
10. Schwartz JC, Younger ST, Nguyen NB, Hardy DB, Monia BP, Corey DR, et al. Antisense transcripts are targets for activating small RNAs. Nat Struct Mol Biol 2008;15:842–8.
11. Modarresi F, Faghihi MA, Lopez-Toledano MA, Fatemi RP, Magistri M, Brothers SP, et al. Inhibition of natural antisense transcripts in vivo results in gene-specific transcriptional upregulation. Nat Biotechnol 2012;30:453–9.
12. el-Deiry WS, Harper JW, O'Connor PM, Velculescu VE, Canman CE, Jackman J, et al. WAF1/CIP1 is induced in p53-mediated G1 arrest and apoptosis. Cancer Res 1994;54:1169–74.
13. Harper JW, Adami GR, Wei N, Keyomarsi K, Elledge SJ. The p21 Cdk-interacting protein Cip1 is a potent inhibitor of G1 cyclin-dependent kinases. Cell 1993;75:805–16.
14. Waga S, Hannon GJ, Beach D, Stillman B. The p21 inhibitor of cyclin-dependent kinases controls DNA replication by interaction with PCNA. Nature 1994;369:574–8.
15. Teraishi F, Kadowaki Y, Tango Y, Kawashima T, Umeoka T, Kagawa S, et al. Ectopic p21sdi1 gene transfer induces retinoic acid receptor beta expression and sensitizes human cancer cells to retinoid treatment. Int J Cancer 2003;103:833–9.
16. Wu M, Bellas RE, Shen J, Sonenshein GE. Roles of the tumor suppressor p53 and the cyclin-dependent kinase inhibitor p21WAF1/CIP1 in receptor-mediated apoptosis of WEHI 231 B lymphoma cells. J Exp Med 1998;187:1671–9.
17. Eastham JA, Hall SJ, Sehgal I, Wang J, Timme TL, Yang G, et al. In vivo gene therapy with p53 or p21 adenovirus for prostate cancer. Cancer Res 1995;55:5151–5.
18. Gao J, Huang HY, Pak J, Cheng J, Zhang ZT, Shapiro E, et al. p53 deficiency provokes urothelial proliferation and synergizes with activated Ha-ras in promoting urothelial tumorigenesis. Oncogene 2004;23:687–96.
19. Mitra AP, Birkhahn M, Cote RJ. p53 and retinoblastoma pathways in bladder cancer. World J Urol 2007;25:563–71.
20. Stein JP, Ginsberg DA, Grossfeld GD, Chatterjee SJ, Esrig D, Dickinson MG, et al. Effect of p21WAF1/CIP1 expression on tumor progression in bladder cancer. J Natl Cancer Inst 1998;90:1072–9.
21. Clasen S, Schulz WA, Gerharz CD, Grimm MO, Christoph F, Schmitz-Drager BJ. Frequent and heterogeneous expression of cyclin-dependent kinase inhibitor WAF1/p21 protein and mRNA in urothelial carcinoma. Br J Cancer 1998;77:515–21.
22. Place RF, Wang J, Noonan EJ, Meyers R, Manoharan M, Charisse K, et al. Formulation of small activating RNA into lipidoid nanoparticles inhibits xenograft prostate tumor growth by inducing p21 expression. Mol Ther Nucleic Acids 2012;1:e15.
23. Karam JA, Huang S, Fan J, Stanfield J, Schultz RA, Pong RC, et al. Upregulation of TRAG3 gene in urothelial carcinoma of the bladder. Int J Cancer 2011;128:2823–32.
24. Semple SC, Akinc A, Chen J, Sandhu AP, Mui BL, Cho CK, et al. Rational design of cationic lipids for siRNA delivery. Nat Biotechnol 2010;28:172–6.
25. Chade DC, Andrade PM, Borra RC, Leite KR, Andrade E, Villanova FE, et al. Histopathological characterization of a syngeneic orthotopic murine bladder cancer model. Int Braz J Urol 2008;34:220–6.
26. Watanabe T, Shinohara N, Sazawa A, Harabayashi T, Ogiso Y, Koyanagi T, et al. An improved intravesical model using human bladder cancer cell lines to optimize gene and other therapies. Cancer Gene Ther 2000;7:1575–80.
27. Chen Z, Place RF, Jia ZJ, Pookot D, Dahiya R, Li LC. Antitumor effect of dsRNA-induced p21(WAF1/CIP1) gene activation in human bladder cancer cells. Mol Cancer Ther 2008;7:698–703.
28. Vaishnaw AK, Gollob J, Gamba-Vitalo C, Hutabarat R, Sah D, Meyers R, et al. A status report on RNAi therapeutics. Silence 2010;1:14.
29. Abbas T, Dutta A. p21 in cancer: intricate networks and multiple activities. Nat Rev Cancer 2009;9:400–14.
30. Gartel AL, Tyner AL. The role of the cyclin-dependent kinase inhibitor p21 in apoptosis. Mol Cancer Ther 2002;1:639–49.
31. Hanke M, Hoefig K, Merz H, Feller AC, Kausch I, Jocham D, et al. A robust methodology to study urine microRNA as tumor marker: microRNA-126 and microRNA-182 are related to urinary bladder cancer. Urol Oncol 2010;28:655–61.
32. Bartlett DW, Su H, Hildebrandt IJ, Weber WA, Davis ME. Impact of tumor-specific targeting on the biodistribution and efficacy of siRNA nanoparticles measured by multimodality in vivo imaging. Proc Natl Acad Sci U S A 2007;104:15549–54.
33. Nogawa M, Yuasa T, Kimura S, Tanaka M, Kuroda J, Sato K, et al. Intravesical administration of small interfering RNA targeting PLK-1 successfully prevents the growth of bladder cancer. J Clin Invest 2005;115:978–85.
34. Seth S, Matsui Y, Fosnaugh K, Liu Y, Vaish N, Adami R, et al. RNAi-based therapeutics targeting survivin and PLK1 for treatment of bladder cancer. Mol Ther 2011;19:928–35.
35. Hadaschik BA, Black PC, Sea JC, Metwalli AR, Fazli L, Dinney CP, et al. A validated mouse model for orthotopic bladder cancer using transurethral tumour inoculation and bioluminescence imaging. BJU Int 2007;100:1377–84.
36. Huang V, Qin Y, Wang J, Wang X, Place RF, Lin G, et al. RNAa is conserved in mammalian cells. PLoS One 2010;5:e8848.

Cancer Research
The Journal of Cancer Research (1916–1930) | The American Journal of Cancer (1931–1940)

AACR American Association for Cancer Research

# Intravesical Delivery of Small Activating RNA Formulated into Lipid Nanoparticles Inhibits Orthotopic Bladder Tumor Growth

Moo Rim Kang, Glen Yang, Robert F. Place, et al.

*Cancer Res* 2012;72:5069-5079. Published OnlineFirst August 6, 2012.